The runaway binary LP 400−22 is leaving the Galaxy

Mukremin Kilic,[1]★ A. Gianninas,[1] Warren R. Brown,[2] Hugh C. Harris,[3]
Conard C. Dahn,[3] M. A. Agüeros,[4] Craig O. Heinke,[5] S. J. Kenyon,[2] J. A. Panei[6]
and Fernando Camilo[4,7]

[1]*Homer L. Dodge Department of Physics and Astronomy, University of Oklahoma, 440 W. Brooks St, Norman, OK 73019, USA*
[2]*Smithsonian Astrophysical Observatory, 60 Garden St, Cambridge, MA 02138, USA*
[3]*US Naval Observatory, Flagstaff Station, 10391 West Naval Observatory Road, Flagstaff, AZ 86001, USA*
[4]*Department of Astronomy, Columbia University, 550 West 120th Street, New York, NY 10027, USA*
[5]*Department of Physics, CCIS 4-183, University of Alberta, Edmonton, AB T6G 2E1, Canada*
[6]*Instituto de Astrofisica La Plata, IALP, CONICET-UNLP, La Plata B1900, Argentina*
[7]*Arecibo Observatory, HC3 Box 53995, Arecibo, PR 00612, USA*

ABSTRACT

We present optical spectroscopy, astrometry, radio and X-ray observations of the runaway binary LP 400−22. We refine the orbital parameters of the system based on our new radial velocity observations. Our parallax data indicate that LP 400−22 is significantly more distant (3σ lower limit of 840 pc) than initially predicted. LP 400−22 has a tangential velocity in excess of 830 km s^{-1}; it is unbound to the Galaxy. Our radio and X-ray observations fail to detect a recycled millisecond pulsar companion, indicating that LP 400−22 is a double white dwarf system. This essentially rules out a supernova runaway ejection mechanism. Based on its orbit, a Galactic Centre origin is also unlikely. However, its orbit intersects the locations of several globular clusters; dynamical interactions between LP 400−22 and other binary stars or a central black hole in a dense cluster could explain the origin of this unusual binary.

Key words: binaries: close − stars: individual: LP 400−22 − stars: individual: WD 2234+222 − white dwarfs − Galaxy: kinematics and dynamics − Galaxy: stellar content.

1 INTRODUCTION

Dynamical processes involving n-body interactions in dense star clusters, supernova explosions in tight binary systems or interactions with the black hole at the Galactic Centre can eject stars from their birthplace at high velocities. In the first scenario, most of the runaway stars ejected from clusters through three-, four- or n-body interactions (Poveda, Ruiz & Allen 1967) are expected to be single stars. However, a small fraction should be tight binaries ejected through close encounters (Gies & Bolton 1986). Binary–binary encounters may disrupt one or both systems, but in 10 per cent of the cases, two binaries are ejected (Mikkola 1983). In the supernova ejection scenario (Blaauw 1961), all runaway binary systems contain the remnant of a supernova explosion, a neutron star or a black hole. However, in the majority of the cases, these companions cannot be detected due to selection effects, e.g. small radial velocity variations due to the low mass of a neutron star compared to the runaway OB stars and the short lifetimes of radio pulsar companions (Portegies Zwart 2000).

Hypervelocity stars (HVSs; Brown et al. 2005, 2007; Edelmann et al. 2005) with velocities even higher than the runaway stars are likely ejected from the Galactic Centre (Hills 1988; Brown et al. 2012). So far, there are no binary HVSs known. However, several HVSs have main-sequence lifetimes significantly shorter than their travel time from the Galactic Centre. Perets (2009) suggests that such stars may be the result of a merger of an HVS binary system that rejuvenates itself after its ejection from the Galactic Centre. HE 0437−5439 (Edelmann et al. 2005; Brown et al. 2010) and US 708 (Hirsch et al. 2005) are two such systems, where the progenitor HVS binaries might have been ejected due to triple disruptions and other dynamical interactions with stars or black holes.

Lu, Yu & Lin (2007) and Sesana, Madau & Haardt (2009) propose that the discovery of HVS binary stars would indicate the existence of a binary black hole at the Galactic Centre. In their model, HVS binaries with velocities ∼1000 km s^{-1} can be ejected from the Galactic Centre due to interactions with a binary black hole. Even though tidal disruption of a hierarchical triple star system by a single black hole may lead to an HVS binary, they find that the ejection rate from this mechanism is negligible (although see the discussion in Perets 2009).

In this paper, we revisit the unusual runaway binary LP 400−22 (WD 2234+222 at $l = 86°.5$ and $b = −30°.7$). Kawka et al. (2006)

★ E-mail: kilic@ou.edu

identified LP 400−22 as a fast moving, extremely low-mass (ELM, 0.17 M$_\odot$) white dwarf (WD) at a distance of 430 ± 45 pc. Kilic et al. (2009) and Vennes et al. (2009) obtained follow-up radial velocity observations, which demonstrated that LP 400−22 is a double degenerate binary system with an orbital period of ≈1 d. Based on the available astrometric data, Kilic et al. (2009) estimated that the probability of a Galactic Centre origin is 0.1 per cent and concluded that LP 400−22 is most likely a halo star with an unusual orbit. Here, we present additional radial velocity, astrometry, X-ray and radio observations of LP 400−22 and revisit its origin. Our observations are discussed in Section 2, whereas the revised binary parameters and its Galactic orbit are discussed in Sections 3 and 4, respectively.

2 OBSERVATIONS

2.1 Optical spectroscopy

We used the 6.5 m MMT equipped with the Blue Channel Spectrograph to obtain additional optical spectroscopy of LP 400−22 over several nights in 2009 September and 2010 November. Our observing and reduction procedures are similar to those of Kilic et al. (2009). The only difference is that most of the new spectra were obtained using a 1.25 arcsec slit, instead of the 1 arcsec slit used in our earlier work.

In addition to measuring radial velocities, we use our MMT data to revise the atmospheric parameters of the visible ELM WD in the system. Fig. 1 shows the fits to the composite spectrum using the pure hydrogen atmosphere models from Tremblay & Bergeron (2009). The best-fitting temperature and gravity with the formal
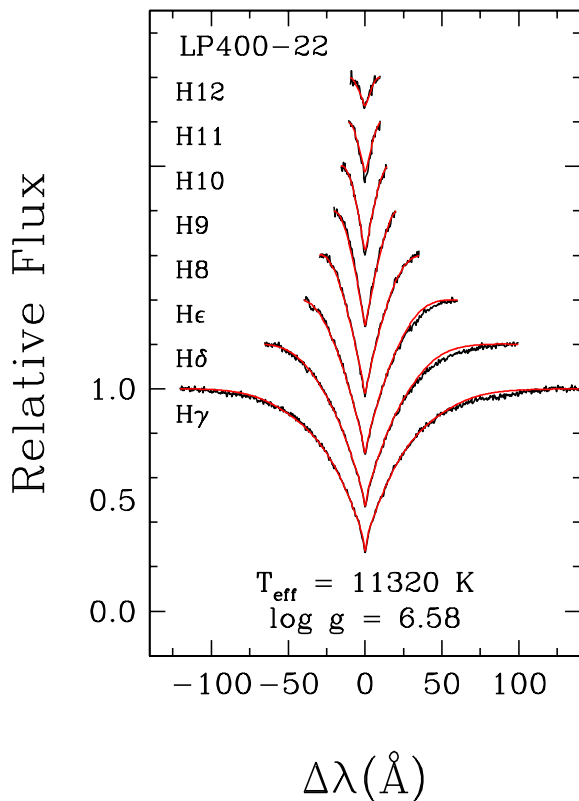

Figure 1. Spectral fits (red lines) to the MMT spectrum (black lines) of LP 400−22.

errors are $T_{\rm eff}$ = 11320 ± 40 K and log g = 6.58 ± 0.01. The best-fitting spectroscopic distance estimate is 350 pc. The temperature estimate is consistent with the previous analysis (Kawka et al. 2006; Kilic et al. 2009; Vennes et al. 2009). However, the gravity estimate is 0.16–0.28 dex higher. The improved Stark broadening profiles of the Tremblay & Bergeron (2009) models lead to an increase of ∼0.1 dex in surface gravity for average mass WDs. We perform a similar analysis of the LP 400−22 spectrum using both old and the new models and find that the new models increase the best-fitting log g estimate by 0.14 dex. Hence, the difference between the previous surface gravity measurements and ours is mostly due to the improved Stark broadening profiles in the new models.

2.2 Astrometry

Astrometric observations of LP 400−22 spanning five seasons were obtained as part of the US Naval Observatory (USNO) parallax programme. Data acquisition and reduction procedures are described in Dahn et al. (2002). Fig. 2 presents the observed parallactic motion for LP 400−22. Using 159 frames taken on 92 nights and 20 reference stars, we measure a relative proper motion of μ = 208.5 ± 0.2 mas yr^{-1} at a position angle of 74°.07 ± 0°.15 and a relative parallax of −0.42 ± 0.30 mas. Using the colours and magnitudes of the reference-frame stars, we estimate the absolute parallax to be 0.26 ± 0.31 mas. Given the relatively small parallax and its large error, we cannot constrain the actual distance to LP 400−22, but we can still use the 3σ lower limit of our parallax measurement to constrain the physical properties of the system. The nominal distance of 3.8 kpc would correspond to a tangential velocity of 3800 km s^{-1}, which is extremely unlikely. The 2σ and 3σ lower limits on the distance are 1130 and 840 pc, respectively. Our proper motion and distance measurements imply a 3σ lower limit on tangential velocity of 830 km s^{-1}, higher than the escape velocity from the Galaxy.

2.3 Radio

We observed LP 400−22 on 2008 March 28 for 22.5 min with the Berkeley-Caltech Pulsar Machine (BCPM; Backer et al. 1997) on the Green Bank Telescope. At the central observing frequency of 820 MHz, the BCPM provided 48 MHz of bandwidth split into 96 spectral channels; for each channel we recorded total power samples every 72 μs. The data reduction was similar to that described in Agüeros et al. (2009b): we used the standard search techniques implemented in the PRESTO software package (Ransom 2001). The dispersion measure range for the search was 0–115 cm^{-3} pc.

We note that while orbital motions can affect the apparent spin period of a pulsar (i.e. if the integration time is a significant fraction of the binary orbital period), here the integration time is only about 1 per cent of the orbital period, so that the assumption of constant apparent acceleration built into PRESTO should hold. No convincing pulsar signal is detected in our data.

2.4 X-ray

We obtained observations of LP 400−22 with *XMM* (ObsID 0553440201, on 2008 November 20) and *Chandra* (ObsID 9962, on 2009 July 28). We analysed the pre-processed (PPS or event2) data sets using SAS v. 11.0 and CIAO v. 4.3. We checked all data for background flares; finding none, we used the whole data sets (livetimes of 1028, 4438, 6520 and 6520 s for *Chandra* ACIS, *XMM* pn, MOS1 and MOS2, respectively). We filtered the *XMM* data sets
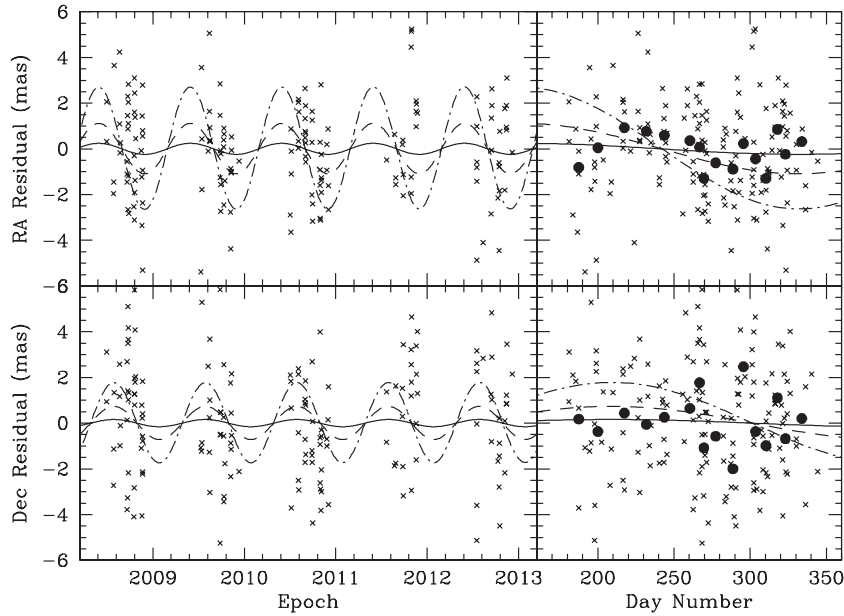
Figure 2. The observed parallactic motion in RA (top panel) and Dec. (bottom panel), after fitting the astrometry for parallax and proper motion, and subtracting the proper motion. The data have the correction to absolute parallax of 0.68 mas added to the observed residuals, as if the reference stars were at infinite distance. The solid curve shows the best-fitting parallax, the dashed fit shows the 3σ upper limit to the parallax and the dot–dashed curve shows the parallax for the spectroscopic distance of 347 pc from Fig. 1. Right-hand panels show the same parallax data folded on a 1 year period, with 10-point means added (filled circles).

following standard procedures:[1] PATTERN $\leq$ 12 and standard FLAG values for the MOS and pn detectors. We created images for each detector in the energy range of 0.5–2 keV.

We calculate the minimum flux expected, should the companion to LP 400−22 be a (recycled) neutron star, with an X-ray luminosity ($L_X(0.3$–2 keV$) = 1.5 \times 10^{30}$ erg cm^{-2} s^{-1}) and spectrum (134 eV blackbody) equal to that of the faintest millisecond pulsar in 47 Tuc (Heinke et al. 2005; Bogdanov, Grindlay & Rybicki 2006; see Agüeros et al. 2009a for the rationale). Assuming a distance of 1.5 kpc and $N_H = 4.5 \times 10^{20}$ cm^{-2}, we predict 0.75, 10, 6 and 6 counts in each detector, using the simulator PIMMS[2] and the exposure times and energy range above.

For the *Chandra* observation, we searched for emission from a 2 arcsec circle centred on LP 400−22's position in the 0.5–2 keV band, but found zero counts. We searched for emission from 10 arcsec circles in the *XMM* images, and we found one event in the pn image and one event in the combined MOS1 and MOS2 image. From *XMM* encircled energy calculations, we find that 60 per cent of the encircled energy should be located within these 10 arcsec extraction regions, so we revise our predicted counts to 6 counts in the searched region of the pn image and 3.6 counts in this region of the combined MOS image. Combining the *XMM* and *Chandra* studied regions, we expect to see 10.4 counts and only see two. Using Poisson statistics (Gehrels 1986), we conclude that we can rule out the hypothesis of a minimal-flux millisecond pulsar at >99.5 per cent confidence, even at the extreme distance of 1.5 kpc. We can rule out millisecond pulsar companions at 90 per cent confidence level out to about 2 kpc. Clearly, LP 400−22 must be within 2 kpc of the Sun for it to have a reasonable tangential velocity of $\leq$2000 km s^{-1}. Therefore, we conclude that the companion must be a WD.

[1] http://heasarc.gsfc.nasa.gov/docs/xmm/abc/
[2] http://asc.harvard.edu/toolkit/pimms.jsp

3 RESULTS

3.1 Orbital parameters

We provide improved orbital parameters of the LP 400−22 binary using the radial velocity measurements from Kilic et al. (2009), Vennes et al. (2009) and our new spectroscopy data. Table 1 lists our 29 new radial velocity measurements. Fig. 3 presents 53 radial velocity measurements obtained over 1500 d and the best-fitting orbit with $P = 1.010\,14(5)$ d, $K = 119.3(8)$ km s^{-1} and systemic velocity $\gamma = -172.0(5)$ km s^{-1}. The revised mass function is $f = 0.1778(36)$. These orbital parameters are consistent with $P = 1.010\,16(5)$ d and $f = 0.180(9)$ from Vennes et al. (2009) within the errors.

3.2 Physical properties

Fig. 4 compares the luminosity, effective temperature and surface gravity of the primary star in LP 400−22 to the evolutionary sequences for 0.15–0.24 M$_\odot$ WDs from Serenelli et al. (2001) and Panei et al. (2007). The 3σ lower limit on distance indicates an absolute magnitude of $M_V = 7.6$ mag, $\log L/L_\odot = -1.05$ and $R = 0.099$ R$_\odot$. These are consistent with the Serenelli et al. (2001) models for a 0.16 M$_\odot$ WD with a thick hydrogen envelope. However, these models predict a surface temperature of 9600 K and $\log g = 5.6$, an order of magnitude lower in surface gravity than the best-fitting model shown in Fig. 1.

Clearly, there is no single model that matches all of the properties of the primary star in LP 400−22. A 0.19 M$_\odot$ WD model can match the best-fitting temperature and surface gravity measurements, but it underpredicts the absolute magnitude, radius and distance. Such a discrepancy between the model and parallax distance measurement for an average mass (0.6 M$_\odot$) DA WD could indicate the existence of spectroscopically invisible helium.

Table 1. New radial velocity measurements for LP 400−22.

HJD−245 5000 (d)	v_{helio} (km s^{-1})
94.815 08	− 102.2 ± 3.8
100.615 35	− 77.1 ± 5.7
100.643 17	− 67.0 ± 4.4
100.650 32	− 61.1 ± 4.8
100.792 41	− 59.8 ± 3.0
101.594 83	− 100.0 ± 5.7
101.599 85	− 97.4 ± 8.4
101.607 01	− 110.2 ± 7.1
101.614 13	− 93.5 ± 5.5
101.622 49	− 81.2 ± 6.9
101.629 61	− 92.3 ± 12.1
101.636 77	− 64.5 ± 5.1
101.872 34	− 89.8 ± 2.4
102.593 03	− 122.3 ± 7.2
102.599 14	− 104.5 ± 5.8
102.607 59	− 100.5 ± 3.9
102.614 94	− 82.6 ± 4.6
102.622 06	− 89.7 ± 3.1
102.630 34	− 95.4 ± 4.7
102.889 91	− 94.6 ± 5.2
511.566 50	− 206.4 ± 8.2
511.580 61	− 204.9 ± 11.9
511.583 08	− 181.4 ± 12.1
511.591 59	− 188.9 ± 9.3
511.594 25	− 172.7 ± 10.1
512.684 15	− 132.4 ± 10.0
512.711 75	− 116.5 ± 6.6
512.754 48	− 85.1 ± 6.8
513.729 02	− 130.7 ± 10.6
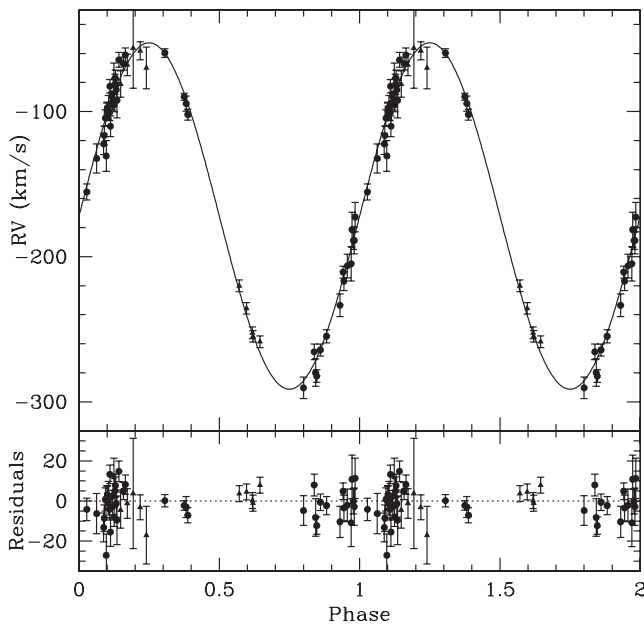
Figure 3. Radial velocity measurements of LP 400−22 from Kilic et al. (2009), Vennes et al. (2009) and this work. The solid line represents the best-fitting model for a circular orbit with a period of 1.010 14 d and $K = 119.3$ km s^{-1}.

Increased pressure broadening of hydrogen lines due to the presence of helium can imitate a higher surface gravity. GD 362 is perhaps the best example of such a system, where the initial model atmosphere analysis showed that the optical spectrum can be explained by a massive (1.2 M$_\odot$) DA WD (Gianninas, Dufour & Bergeron 2004). However, follow-up high-resolution observations (Zuckerman et al. 2007) and a parallax measurement (Kilic, Thorstensen & Koester 2008) showed that GD 362 indeed has a helium-dominated atmosphere and that it is not a massive WD. Since He becomes transparent below about 11 000 K, it is possible to hide significant amounts of He in the atmosphere of LP 400−22. To investigate this possibility and to check whether a mixed H/He atmosphere solution would give results consistent with the parallax measurement, we computed model atmospheres with He/H ratios ranging from 0 to 100.

Fig. 5 shows the Balmer line profiles of LP 400−22 compared to mixed atmosphere models with $T_{eff} = 9600$ K, log $g = 5.6$ (see the above discussion) and He/H = 0, 1, 10 and 20. None of these models provide a reasonable fit to the observed spectrum of LP 400−22. This is because the addition of helium to a log $g = 6$ atmosphere does not have the same effect as that of a log $g = 8$ or 9 atmosphere. In addition, the spectral energy distribution analysis of Kawka et al. (2006) using ultraviolet and optical photometry is in excellent agreement with the Balmer line analysis using pure H models. Hence, a temperature as low as 9600 K can be ruled out from both spectroscopy and photometry.

Fig. 6 shows the temperature, pressure and Balmer line profiles of mixed H/He atmosphere models with He/H = 20 and log $g = 6$, 7, 8 and 9. The pressure for the log $g = 6$ model is two orders of magnitude smaller than it is for the log $g = 9$ model. The results are similar for models with different He/H ratios, e.g. He/H = 50, 100. Hence, the effect of helium on the atmospheric structure and the Balmer line profiles is negligible for low-surface-gravity models appropriate for ELM WDs, including LP 400−22. Figs 5 and 6 demonstrate that the addition of He in our spectral models for LP 400−22 does not resolve the discrepancy between the observed properties and the evolutionary models.

An alternative explanation for the discrepancy in the spectroscopic distance estimate is an unresolved DA + DC WD system, where the DC WD companion is bright enough to contribute to the spectral continuum, but not to the Balmer line profiles. We tested this scenario by fitting the observed spectrum as a composite DA + DC system. We fixed the log g of the DC component to log $g = 7.5$ or 7.7 (0.4 or 0.5 M$_\odot$) and allowed the other three parameters, temperature and surface gravity of the DA component and the temperature of the DC component, to vary. Our fitting algorithm achieves a good fit to the observed spectrum only if the DC component is cool enough ($T_{eff} < 3500$ K) that it essentially does not contribute any light to the system. We do not find any plausible solutions involving a composite DA + DC spectrum.

Althaus, Serenelli & Benvenuto (2001) and Serenelli et al. (2001) predict that $M \geq 0.2$ M$_\odot$ WDs suffer from diffusion-induced hydrogen shell flashes that lead to thin hydrogen envelopes. The surface gravity and temperature measurements for LP 400−22 place it right in the transition region between the objects with and without hydrogen shell flashes (see Fig. 3). Panei et al. (2007) argue that the lower mass limit for shell flashes is 0.17 M$_\odot$. Below this mass limit, WDs have a thick hydrogen surface layer that provides energy through stable hydrogen burning. This extra energy source slows down the evolution of the lowest mass WDs, keeping them luminous for longer than expected. Based on the Panei et al. (2007) models, the temperature and surface gravity measurements for
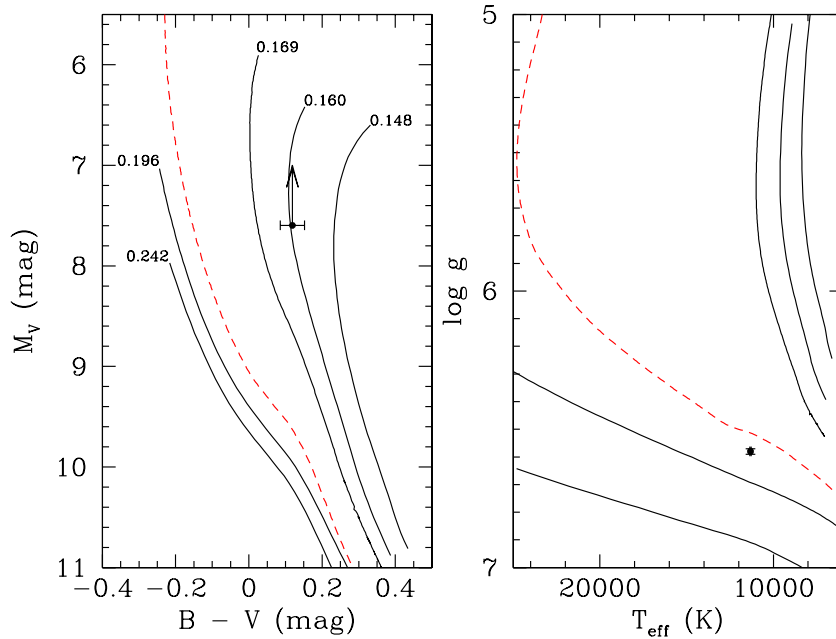
Figure 4. LP 400−22 on a colour–magnitude diagram (left) and a T_{eff} versus log g diagram. Evolutionary model sequences for 0.15–0.24 M$_\odot$ He-core WDs (solid lines; Serenelli et al. 2001) and 0.19 M$_\odot$ WDs (dashed lines; Panei et al. 2007) are also shown.
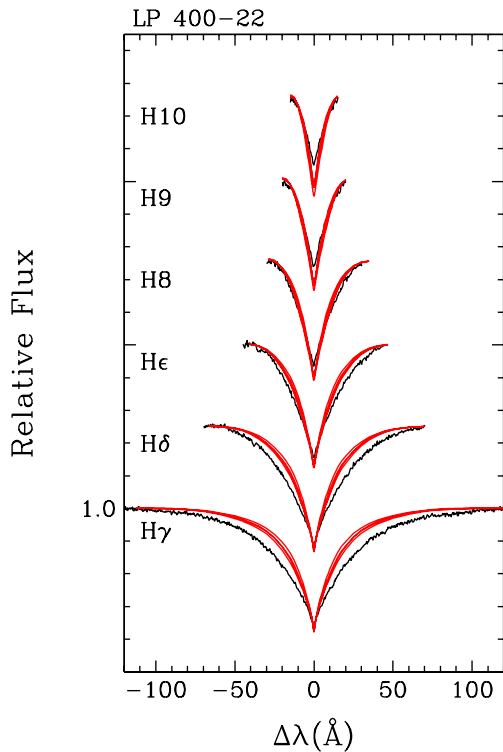

Figure 5. The MMT spectrum (black lines) of LP 400−22 compared to mixed atmosphere models with $T_{eff} = 9600$ K, log $g = 5.6$ and He/H = 0, 1, 10 and 20 (from top to bottom, red lines). The Balmer line profiles for these mixed atmosphere models are essentially identical to each other due to the low surface gravity.

LP 400−22 imply an ≈0.19 M$_\odot$ WD with a thin H envelope of log $M/M_\star = -3.1$. On the other hand, its luminosity and colours do not match any of the Panei et al. (2007) cooling tracks; LP 400−22 may be a pre-WD.

The mass estimate for LP 400−22 ranges from 0.16 to 0.19 M$_\odot$. The observed parallax implies that LP 400−22 is significantly more luminous than initially predicted from the models. However, given the uncertainties in models and specifically the transition from hydrogen shell flashes to stably burning envelopes for ≈0.2 M$_\odot$ WDs, it is perhaps not surprising to find discrepancies between the model expectations and the observed properties. Regardless of these issues, the observed surface gravity of the primary star in LP 400−22 shows that it is clearly a WD, and its brightness suggests that it is likely to have a thick envelope with stable hydrogen burning.

We note that the ELM WD in the eclipsing double WD binary NLTT 11748 (Steinfadt et al. 2010) looks like a cooler version of the primary star in LP 400−22. NLTT 11748 has essentially the same surface gravity as LP 400−22, but the primary WD has $T_{eff} = 8690 \pm 140$ K. NLTT 11748 was also observed as part of the USNO parallax programme, and the distance measurement agrees with model expectations for that star (Harris, private communication). Hence, the difference between the NLTT 11748 and LP 400−22 ELM WDs may be a slight difference in mass and a significant difference in the thickness of the surface hydrogen layer.

3.3 The galactic orbit

The lack of a signature of a millisecond pulsar companion in the radio and X-ray observations demonstrates that LP 400−22 is a double WD binary system containing an ELM WD and an invisible higher mass ($M \geq 0.39$ M$_\odot$) WD companion at an inclination larger than 33°.

Fig. 7 presents its Galactic orbit assuming a static disc–halo–bulge potential (Kenyon et al. 2008), 250 km s^{-1} solar rotation (Reid et al. 2009), the local standard of rest as defined by Schönrich, Binney & Dehnen (2010) and $X = 8$ kpc and $Z = 20$ pc for the location of the Sun (Reed 2006). Even at the 3σ lower limit of 840 pc, LP 400−22 is unbound.
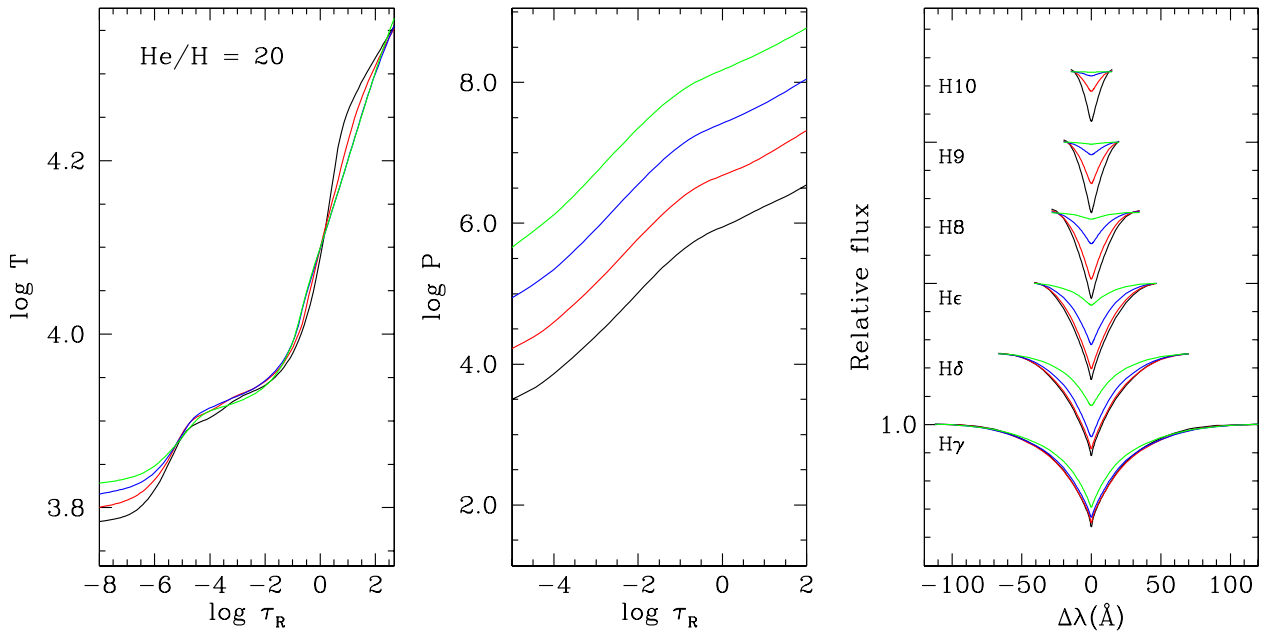
Figure 6. Temperature (left), pressure (middle) and Balmer line profiles (right) of model atmospheres with He/H = 20, T_{eff} = 11 500 K and log g = 6–9 (from bottom to top).
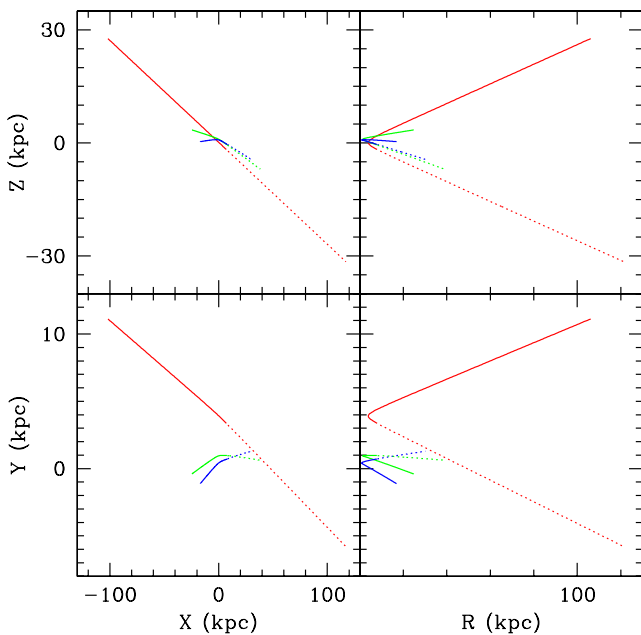

Figure 7. Galactic orbit of LP400−22 for a distance of 3800 pc (red), 1130 pc (green, 2σ lower limit) and 840 pc (blue, 3σ lower limit). The solid and dotted lines show the past and future orbits for 30 Myr.

For the three trajectories shown in Fig. 7, the closest pericentre passage occurs 2–9 Myr ago at distances of 0.9–3.9 kpc. Hence, a Galactic Centre origin is effectively ruled out for LP 400−22. The main problem is that the W component of the velocity, −140 (−220) km s^{-1} for the 3σ (2σ) lower limit on distance, is too large for a trajectory originating in the Galactic Centre. We note that the use of a different Galactic potential, i.e. that of Gnedin et al. (2005), does not change any of our conclusions.

4 DISCUSSION

LP 400−22 is an unbound runaway binary WD system. There are other binary runaway systems known; roughly 5–26 per cent of runaway O-type stars are binary systems (Mason et al. 1998). However, LP 400−22 is unique, since it is the only runaway binary WD system currently known and it has an extremely large space velocity compared to typical runaway stars.

Unlike the neutron star companions to OB stars, a neutron star companion to LP 400−22 should be detected as a recycled millisecond pulsar through radial velocity, radio and X-ray observations. Our observations indicate that LP 400−22 binary has a circular orbit with no evidence of a neutron star companion. In addition, <1 per cent of runaways are expected to receive velocity kicks in excess of 200 km s^{-1} (Portegies Zwart 2000). The observed space velocity of LP 400−22 and the non-detection of a neutron star companion indicate that the supernova ejection mechanism cannot explain the origin of the LP 400−22 binary.

Hypervelocity binary systems may form due to the tidal disruption of a hierarchical triple star by the central black hole or the interaction of a binary star with a binary black hole at the Galactic Centre. Lu et al. (2007) estimate that the latter formation channel can form hypervelocity binary systems with velocities up to 1000 km s^{-1}. However, LP 400−22 has a Galactic orbit that is inconsistent with a Galactic Centre origin. Hence, the Galactic Centre ejection mechanism through interactions with the central black hole(s) also cannot explain the origin of the LP 400−22 binary.

An alternative birthplace where interactions with an intermediate-mass black hole can take place and the number density of the stellar population is high enough for frequent close encounters is globular clusters. Multibody interactions in a dense star cluster can in principle explain the origin of LP 400−22. Some runaway stars can be traced back to their birthplace because of their short main-sequence lifetimes and their proximity to known clusters, associations or H II regions. In the case of LP 400−22, its WD age and total age are uncertain, and there is no way to confirm its birthplace given the
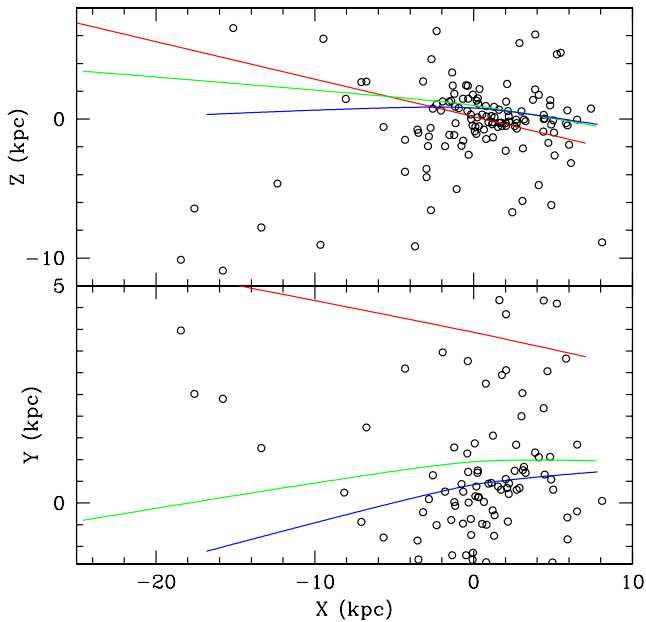
Figure 8. Galactic orbit of LP400−22 for the past 30 Myr. The symbols are the same as in Fig. 7. The open circles show the positions of the known globular clusters.

uncertainties in its distance measurement. Nevertheless, an origin in a globular cluster is possible.

Fig. 8 shows the Galactic orbit for LP 400−22 for the past 30 Myr along with the positions of the known globular clusters (Harris 1996). For a distance of 840 pc, 4.2 Myr ago LP 400−22 was within 170 pc of the globular cluster 2MASS-GC01. Given the uncertainties in distance, it is not possible to locate the cluster that LP 400−22 definitely came from. However, this figure demonstrates that there are several globular clusters in the vicinity of LP 400−22's trajectory that may explain its origin.

There are only a handful of HVSs with accurate proper motion measurements. The problem is that many of them are located at ∼100 kpc; space-based telescopes are required to measure their proper motion. Brown et al. (2010) used the *Hubble Space Telescope* to measure the proper motion of the HVS HE 0437−5439 and demonstrated that its velocity vector points directly away from the Galactic Centre. Similar observations of the other known HVSs are required to directly link them to the Galactic Centre.

There are two cases where accurate proper motions are available and they are inconsistent with a Galactic Centre origin. HD 271791 is an 11 M$_\odot$ B-type star with a velocity larger than the Galactic escape velocity. Heber et al. (2008) show that its kinematic properties rule out a Galactic Centre origin, and they are more consistent with the formation in the outer disc. Similarly, SDSS J013655.91+242546.0 is a 2.5 M$_\odot$ A-type main-sequence star, likely unbound to the Galaxy and with an origin near the outer Galactic disc (Tillich et al. 2009). LP 400−22 joins this group of runaway stars for which a Galactic Centre origin is ruled out based on proper motion measurements.

Gualandris & Portegies Zwart (2007) and Gvaramadze, Gualandris & Portegies Zwart (2008) argue that close encounters between two hard binaries or interactions with an intermediate-mass (∼10^3 M$_\odot$) black hole in a dense environment can explain HVSs like HE 0437−5439, assuming that it originated in a star cluster in the Large Magellanic Cloud (LMC). Even though we now know that HE 0437−5439 did not originate in the LMC (Brown

et al. 2010), the same arguments can be used to explain the origin of the LP 400−22 binary system in a Milky Way globular cluster. Hard binary interactions can eject single stars with velocities up to 1400 km s^{-1} (Leonard 1991). The ejection velocity can be as large as 2300 km s^{-1}, if the binaries involved in the interaction consist of low-mass systems that have already gone through common-envelope evolution (Gvaramadze et al. 2008). Even though detailed dynamical simulations for the LP 400−22 binary are currently not available, it is likely that LP 400−22 formed through multibody interactions involving hard binaries and/or an intermediate-mass black hole in a dense cluster.

5 CONCLUSIONS

We refine the orbital parameters of the intriguing runaway binary WD LP 400−22. Based on our parallax measurements, we demonstrate that this binary is unbound to the Galaxy. We estimate its Galactic orbit using a static disc–halo–bulge potential and find a Galactic Centre origin unlikely. No neutron star companion is detected in the radio and X-ray data, indicating that a supernova ejection mechanism is ruled out for this system. The only remaining explanation for the unusual space velocity of LP 400−22 is multibody interactions involving hard binary systems or the disruption of a hierarchical triple system by an intermediate-mass black hole in a dense cluster. LP 400−22's trajectory intersects several known globular clusters. However, due to the relatively uncertain distance measurement, we cannot link LP 400−22 with any single globular cluster. Further follow-up parallax observations at the USNO and with the *GAIA* satellite will be extremely helpful in constraining the Galactic orbit for LP 400−22. In addition, dynamical simulations specifically designed to study the LP 400−22 binary WD system will be useful for understanding its origin in a dense cluster and its implications for the existence of intermediate-mass black holes in globular clusters.

NOTE ADDED IN PRESS

We are continuing to observe LP 400-22 as part of the USNO parallax programme. Observations obtained over the summer of 2013 confirm the parallax measurement presented in this paper (Dahn, private communication).

REFERENCES

Agüeros M. A., Camilo F., Silvestri N. M., Kleinman S. J., Anderson S. F., Liebert J. W., 2009a, ApJ, 697, 283

Agüeros M. A. et al., 2009b, ApJ, 700, L123

Althaus L. G., Serenelli A. M., Benvenuto O. G., 2001, MNRAS, 323, 471

Backer D. C., Dexter M. R., Zepka A., Zepka A., Ng D., Werthimer D. J., Ray P. S., Foster R. S., 1997, PASP, 109, 61

Blaauw A., 1961, Bull. Astron. Inst. Netherlands, 15, 265

Bogdanov S., Grindlay J. E., Rybicki G. B., 2006, ApJ, 648, L55

Brown W. R., Geller M. J., Kenyon S. J., Kurtz M. J., 2005, ApJ, 622, L33

Brown W. R., Geller M. J., Kenyon S. J., Kurtz M. J., Bromley B. C., 2007, ApJ, 671, 1708

Brown W. R., Anderson J., Gnedin O. Y., Bond H. E., Geller M. J., Kenyon S. J., Livio M., 2010, ApJ, 719, L23

Brown W. R., Cohen J. G., Geller M. J., Kenyon S. J., 2012, ApJ, 754, L2

Dahn C. C. et al., 2002, AJ, 124, 1170

Edelmann H., Napiwotzki R., Heber U., Christlieb N., Reimers D., 2005, ApJ, 634, L181

Gehrels N., 1986, ApJ, 303, 336

Gianninas A., Dufour P., Bergeron P., 2004, ApJ, 617, L57

Gies D. R., Bolton C. T., 1986, ApJS, 61, 419

Gnedin O. Y., Gould A., Miralda-Escudé J., Zentner A. R., 2005, ApJ, 634, 344

Gualandris A., Portegies Zwart S., 2007, MNRAS, 376, L29

Gvaramadze V. V., Gualandris A., Portegies Zwart S., 2008, MNRAS, 385, 929

Harris W. E., 1996, AJ, 112, 1487

Heber U., Edelmann H., Napiwotzki R., Altmann M., Scholz R.-D., 2008, A&A, 483, L21

Heinke C. O., Grindlay J. E., Edmonds P. D., Cohn H. N., Lugger P. M., Camilo F., Bogdanov S., Freire P. C., 2005, ApJ, 625, 796

Hills J. G., 1988, Nat, 331, 687

Hirsch H. A., Heber U., O'Toole S. J., Bresolin F., 2005, A&A, 444, L61

Kawka A., Vennes S., Oswalt T. D., Smith J. A., Silvestri N. M., 2006, ApJ, 643, L123

Kenyon S. J., Bromley B. C., Geller M. J., Brown W. R., 2008, ApJ, 680, 312

Kilic M., Thorstensen J. R., Koester D., 2008, ApJ, 689, L45

Kilic M., Brown W. R., Allende Prieto C., Swift B., Kenyon S. J., Liebert J., Agüeros M. A., 2009, ApJ, 695, L92

Leonard P. J. T., 1991, AJ, 101, 562

Lu Y., Yu Q., Lin D. N. C., 2007, ApJ, 666, L89

Mason B. D., Gies D. R., Hartkopf W. I., Bagnuolo W. G., Jr, ten Brummelaar T., McAlister H. A., 1998, AJ, 115, 821

Mikkola S., 1983, MNRAS, 203, 1107

Panei J. A., Althaus L. G., Chen X., Han Z., 2007, MNRAS, 382, 779

Perets H. B., 2009, ApJ, 698, 1330

Portegies Zwart S. F., 2000, ApJ, 544, 437

Poveda A., Ruiz J., Allen C., 1967, Bol. Obs. Tonantzintla Tacubaya, 4, 86

Ransom S. M., 2001, BAAS, 33, 119.03

Reed B. C., 2006, J. R. Astron. Soc. Can., 100, 146

Reid M. J. et al., 2009, ApJ, 700, 137

Schönrich R., Binney J., Dehnen W., 2010, MNRAS, 403, 1829

Serenelli A. M., Althaus L. G., Rohrmann R. D., Benvenuto O. G., 2001, MNRAS, 325, 607

Sesana A., Madau P., Haardt F., 2009, MNRAS, 392, L31

Steinfadt J. D. R., Kaplan D. L., Shporer A., Bildsten L., Howell S. B., 2010, ApJ, 716, L146

Tillich A., Przybilla N., Scholz R.-D., Heber U., 2009, A&A, 507, L37

Tremblay P.-E., Bergeron P., 2009, ApJ, 696, 1755

Vennes S., Kawka A., Vaccaro T. R., Silvestri N. M., 2009, A&A, 507, 1613

Zuckerman B., Koester D., Melis C., Hansen B. M., Jura M., 2007, ApJ, 671, 872

This paper has been typeset from a TEX/LATEX file prepared by the author.